American Mineralogist, Volume 88, pages xxx–xxx, 2003

An X-ray Rietveld, infrared, and Mössbauer spectral study of the $NaMn(Fe_{1-x}In_x)_2(PO_4)_3$ alluaudite-type solid solution

FRÉDÉRIC HATERT,[1] RAPHAËL P. HERMANN,[2] GARY J. LONG,[3] ANDRÉ-MATHIEU FRANSOLET,[1] AND FERNANDE GRANDJEAN[2]

[1]Laboratoire de Minéralogie, B18, Université de Liège, B-4000 Sart-Tilman, Belgium
[2]Institut de Physique, B5, Université de Liège, B-4000 Sart-Tilman, Belgium
[3]Department of Chemistry, University of Missouri-Rolla, Missouri 65409-010, U.S.A.

ABSTRACT

Several compounds of the $NaMn(Fe_{1-x}In_x)_2(PO_4)_3$ solid solution were synthesized by solid state reaction in air; pure alluaudite-like compounds were obtained for $x = 0.00$ to 1.00. X-ray Rietveld refinements indicate the presence of Na^+ at the A1 and A2' sites, Mn^{2+} at the M1 site, and Fe^{2+}, Fe^{3+}, and In^{3+} at the M2 site. The presence of small amounts of In^{3+} at the M1 site, and Mn^{2+} at the M2 site, indicates a partially disordered distribution between these cations. A good correlation was also established between the M1-M2 bond distance and the β angle of the alluaudite-like compounds. The disordered distribution of Fe^{2+}, Fe^{3+}, and In^{3+} at the M2 site is confirmed by the broadness of the infrared absorption bands. The Mössbauer spectra, measured between 90 and 295 K, were analyzed in terms of a model that takes into account the next-nearest neighbor interactions around the M2 crystallographic site. In all cases these spectra reveal the unexpected presence of small amounts of Fe^{2+} at the M2 site, an amount that decreases as the In^{3+} content increases. The Fe^{2+} and Fe^{3+} isomer shifts are typical of the alluaudite structure and vary with temperature, as expected from a second-order Doppler shift. The derived iron vibrating masses and Mössbauer lattice temperatures are within the expected range of values for iron cations in an octahedral environment. The Fe^{2+} and Fe^{3+} quadrupole splittings are also typical of the alluaudite structure and the temperature dependence of the Fe^{2+} quadrupole splitting was fit with the model of Ingalls (1964), which yielded a ground state orbital splitting of ca. 380 to 570 cm^{-1} for the Fe^{2+} sites.

INTRODUCTION

The alluaudite mineral group consists of Na-Mn-Fe-bearing phosphates that are known to occur in granitic pegmatites, particularly in the beryl-columbite-phosphate subtype of the rare-element pegmatites, according to the classification of Černý (1991). Wyllieite and bobfergusonite are two pegmatite phosphates homeotypic with alluaudite.

Moore (1971) determined the crystal structure of alluaudite in the monoclinic *C2/c* space group and derived the general structural formula $X2X1M1M2_2(PO_4)_3$, with $Z = 4$. The structure consists of kinked chains of edge-sharing octahedra stacked parallel to {101}. These chains are formed by a succession of M2 octahedral pairs linked by highly distorted M1 octahedra. Equivalent chains are connected in the *b* direction by the P1 and P2 phosphate tetrahedra to form sheets oriented perpendicular to [010]. These interconnected sheets produce channels parallel to **c**, channels that contain the distorted cubic X1 site and the four-coordinated X2 site.

The past decade has seen an increasing number of structural studies of synthetic phosphates with the alluaudite structure. These papers (Yakubovich et al. 1977; Antenucci 1992; Warner et al. 1993; Antenucci et al. 1995; Leroux et al. 1995a, 1995b; Lii and Ye 1997; Korzenski et al. 1998; Hatert et al. 2000; Chouaibi et al. 2001) clearly demonstrate the existence of three cationic sites in the alluaudite structure, sites that were not reported by Moore (1971). These sites are located in the channels at crystallographic positions different from X1 and X2. Based on detailed structural studies, Hatert et al. (2000) proposed a new general formula, $(A2A2')(A1A1'A1''_2)M1M2_2(PO_4)_3$, for alluaudite-type compounds.

In granitic pegmatites, alluaudite displays chemical compositions mainly varying between the two end-members, $Na_2Mn(Fe^{2+}Fe^{3+})(PO_4)_3$ and $\square NaMnFe^{3+}_2(PO_4)_3$, with Mn^{2+} or some Ca^{2+} replacing Na^+ at the A1 site, Fe^{2+} replacing Mn^{2+} at the M1 site, and Mg^{2+} or Mn^{2+} replacing Fe at the M2 site, where $\square$ represents a lattice vacancy at the A2' site. Because of the complex chemical compositions of natural alluaudite minerals, pure alluaudite-like compounds have been synthesized in order to better understand the crystal chemistry of the alluaudite structure. Whereas the crystallochemical role of lithium was investigated by Hatert et al. (2000, 2001) and Hermann et al. (2001), the crystal chemistry of the trivalent cation has only been briefly investigated by Antenucci (1992) who synthesized $Na_2Cd_2M(PO_4)_3$, where M is Fe^{3+}, Cr^{3+}, or Ga^{3+}. A large number of indium-bearing alluaudite-like compounds have also been synthesized, i.e., $NaCdIn_2(PO_4)_3$ (Antenucci et al. 1993), $Na_3In_2(PO_4)_3$ (Lii and Ye 1997), and $Na_3In_2(AsO_4)_3$ (Lii and Ye 1997; Khorari et al. 1997). The similarities between In^{3+} and the trivalent transition metal cat-

* E-mail: fhatert@ulg.ac.be

0003-004X/03/0001–xxx$05.00

ions led to the synthesis of mixed indium-iron phosphates by Tang et al. (1999).

In order to better understand the structural and electronic consequences of the replacement of Fe^{3+} by In^{3+} in the alluaudite structure, a study of the $NaMn(Fe_{1-x}In_x)_2(PO_4)_3$ solid solution has been carried out by X-ray diffraction and infrared and Mössbauer spectroscopies. Mössbauer spectroscopy is an especially valuable tool for this study because it provides information about the cation distributions at the M1 and M2 crystallographic sites, distributions that govern the transition from the disordered alluaudite structure to the more ordered wyllieite (Moore and Molin-Case 1974) and bobfergusonite (Ercit et al. 1986) structures.

Experimental methods

Compounds of the $NaMn(Fe_{1-x}In_x)_2(PO_4)_3$ series, with x ranging from 0.00 and 1.00, have been synthesized through a solid state reaction carried out in air. Stoichiometric quantities of $NaHCO_3$, MnO, $FeSO_4{\cdot}7H_2O$, In_2O_3, and $(NH_4)H_2PO_4$ were dissolved in concentrated nitric acid and the resulting solution was evaporated to dryness. The dry residue was progressively heated in a platinum crucible, at a heating rate of 500°/hour, to either 900 or 1000 °C, and was then maintained at this temperature for 13 to 16 hours. Alluaudite-like compounds were obtained by quenching the product in air.

X-ray powder diffraction patterns of the compounds were recorded with a diffractometer using Fe$K\alpha$ 1.9373 Å radiation. The unit-cell parameters (Table 1) were calculated with the least-squares refinement program LCLSQ 8.4 (Burnham 1991) from the d spacings calibrated with $Pb(NO_3)_2$ as an internal standard.

Wet chemical analyses of the synthetic alluaudite crystals (Table 2) were performed on 57 to 117 mg of material. Atomic absorption spectrophotometry was used to determine the sodium, manganese, and total iron content, whereas the phosphorus content was determined by colorimetry. The Ungethüm method (Ungethüm 1965) was used to determine of Fe^{2+}, and the indium content was calculated from the theoretical composition.

The X-ray Rietveld refinements of $NaMn(Fe_{1-x}In_x)_2(PO_4)_3$, with x = 0.25, 0.50, 0.75, and 1.00, were carried out with data collected on a Philips PW-3710 diffractometer with Fe$K\alpha$ radiation. The unit-cell parameters calculated from the $Pb(NO_3)_2$-calibrated powder pattern (Table 1), and the atomic positions reported for $NaMnFe_2(PO_4)_3$ (Hatert et al. 2000), served as starting parameters for the refinements that were performed with the DBWS-9807 program developed by Young et al. (1998). The investigated 2θ range extended from 10 to 100°, the step width was 0.02°, and the step time was 15 s. The total number of refined parameters was 55 with 504, 510, 524, and 530 observed reflections, for x = 0.25, 0.50, 0.75, and 1.00, respectively. The final Rietveld plot for $NaMnFeIn(PO_4)_3$ is shown in Figure 1. Fits of equivalent quality were obtained for the other compounds.

Infrared spectra were recorded with either a Nicolet MAGNA-IR 760 spectrometer over the 400–4000 cm^{-1} range using KBr discs, or a Bruker IFS 66 spectrometer over the 100–550 cm^{-1} range using polyethylene discs.

Mössbauer spectra were measured between 90 and 295 K with a constant-acceleration spectrometer that utilized a room temperature rhodium matrix ^{57}Co source and was calibrated at room temperature with α-iron foil. The Mössbauer spectral absorbers contained 30, 34, 36, 18, 22, and 13 mg/cm² of powder for x = 0.00, 0.10, 0.25, 0.50, 0.75, and 0.90, respectively. $NaMn^{57}Fe_{0.02}In_{1.98}(PO_4)_3$ was prepared with 95% enriched ^{57}Fe and its absorber contained 32 mg/cm² of sample.

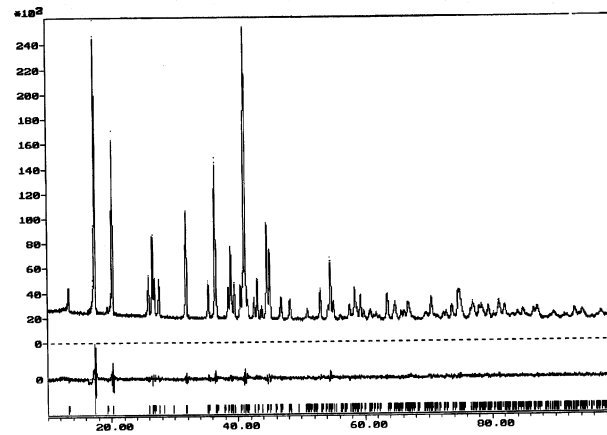

Figure 1. The observed (dots), calculated (solid line), and difference X-ray powder diffraction patterns of $NaMnFeIn(PO_4)_3$ obtained from a Rietveld refinement. The vertical markers indicate the positions calculated for the Fe$K\alpha_1$ and Fe$K\alpha_2$ Bragg reflections.

Table 1. Unit-cell parameters for the synthetic alluaudite-like compounds, $NaMn(Fe_{1-x}In_x)_2(PO_4)_3$ (space group $C2/c$)

x	a (Å)	b (Å)	c (Å)	β (°)	V (Å³)
0.00	12.001(2)	12.538(2)	6.405(1)	114.45(1)	877.3(2)
0.10	12.013(2)	12.572(3)	6.416(1)	114.45(2)	882.1(2)
0.25	12.064(2)	12.641(2)	6.428(1)	114.63(1)	891.2(2)
0.50	12.131(2)	12.746(2)	6.470(1)	114.84(1)	907.9(2)
0.75	12.222(3)	12.845(2)	6.507(1)	115.11(2)	925.0(2)
0.90	12.261(3)	12.911(2)	6.535(1)	115.20(2)	936.1(2)
1.00	12.282(2)	12.948(2)	6.552(1)	115.21(1)	942.8(2)

Table 2. Chemical analyses of the alluaudite-like compounds, $NaMn(Fe_{1-x}In_x)_2(PO_4)_3$

x	0.00	0.10	0.25	0.50	0.75	0.90	1.00
P_2O_5	44.41	43.49	40.47	38.13	36.35	38.28	35.49
In_2O_3 (*)	–	5.67	13.19	24.86	35.55	44.92	46.28
Fe_2O_3	30.05	27.43	23.60	14.75	7.53	2.89	–
FeO	3.62	3.15	1.59	0.91	0.00	0.00	–
MnO	15.93	14.76	13.99	13.11	12.48	12.11	11.75
Na_2O	6.11	6.13	6.04	5.76	5.40	5.99	5.09
Total	100.12	100.63	98.88	97.52	97.31	104.19	98.61
Cation numbers							
P	3.000	3.000	3.000	3.000	3.000	3.000	3.000
In (*)	–	0.200	0.500	1.000	1.500	1.800	2.000
Fe^{3+}	1.804	1.682	1.555	1.032	0.552	0.201	–
Fe^{2+}	0.242	0.215	0.116	0.071	0.000	0.000	–
Mn	1.077	1.019	1.038	1.032	1.030	0.950	0.994
Na	0.945	0.968	1.025	1.038	1.021	1.075	0.985
Fe^{3+} (%)	88.2	88.7	93.0	93.6	100.0	100.0	–
Fe^{2+} (%)	11.8	11.3	7.0	6.4	0.0	0.0	–

Note: Wet chemical analyses by J.-M. Speetjens. Cation numbers were calculated on the basis of 3 P per formula unit, and the In content (*) was deduced from the theoretical composition.

CRYSTAL CHEMISTRY OF $NaMn(Fe_{1-x}In_x)_2(PO_4)_3$

Characterization of the compounds

The $NaMn(Fe_{1-x}In_x)_2(PO_4)_3$ alluaudite-like compounds crystallize as fine-grained white powders. Powder X-ray diffraction patterns indicate that pure alluaudite-like phases are obtained for all x values between 0.00 and 1.00. The wet chemical analyses (Table 2) confirm the chemical composition of the compounds and indicate the presence of 0.0 to 11.8 atomic percent of Fe^{2+}, an amount that decreases as x increases.

X-ray Rietveld refinements

The reliability factors, positional parameters, site occupancies, and interatomic distances and angles, deduced from the Rietveld refinements of the X-ray powder diffraction patterns of the $NaMn(Fe_{1-x}In_x)_2(PO_4)_3$ alluaudite-like compounds, are given in Tables 3, 4, and 5, respectively. Both the satisfactory values of R_p, R_{wp}, R_{Bragg}, and S (Table 3), and the mean O-P1-O and O-P2-O angles (Table 5), which are close to those of an ideal tetrahedron, confirm the reliability of the refinements. A polyhedral representation of the crystal structure of $NaMnFeIn(PO_4)_3$, projected along the approximate [001] direction, is shown in Figure 2.

The crystallographic sites of the alluaudite-like compounds (Table 4) are labeled according to the nomenclature recently proposed by Hatert et al. (2000). The morphologies of the coordination polyhedra of M1 and M2 are those of distorted octahedra, whereas the morphologies of A1 and A2' are those of a distorted cube and of a gabled disphenoid, respectively. These morphologies are similar to those previously described for the $(Na_{1-x}Li_x)MnFe_2(PO_4)_3$ compounds (Hatert et al. 2000).

The occupancy factors given in Table 4 indicate that the A1 site is filled with Na^+, whereas the A2' site contains only small amounts of this cation. This distribution of Na^+ between the A1 and A2' crystallographic sites is similar to that already observed for $NaMnFe_2(PO_4)_3$ (Hatert et al. 2000). The positions of the sodium atom at the A2' site are shown in Figure 3. For x = 0.25 and 0.50, Na^+ is located above the square formed by the four O6 atoms, whereas for x = 0.75, Na^+ is located below this plane.

Because Fe^{3+} and Mn^{2+} cannot be distinguished by Rietveld refinements of X-ray data, the Fe^{3+}-content of the M2 site was fixed to its theoretical value. Preliminary refinements were performed assuming Mn^{2+} at M1 and (Fe^{3+}, In^{3+}) at M2. These refinements showed a rather high electronic density at M1, whereas the electronic density at M2 was particularly low, compared to the theoretical values. This behavior is likely related to the presence of small amounts of In^{3+} at the M1 site and of Mn^{2+} at the M2 site. Consequently, the occupancy factors for the M sites (Table 4) were calculated assuming a full occupancy of M1 by Mn^{2+} and In^{3+}, and of M2 by Fe^{3+}, In^{3+}, and Mn^{2+}.

The partially disordered cationic distribution of Mn^{2+} and In^{3+} at the M1 and M2 crystallographic sites is probably due to the similar ionic radii of Mn^{2+} and In^{3+}, 0.830 and 0.800 Å, respectively (Shannon 1976). As is shown in Figure 4, In^{3+} occupies the M1 site up to a maximum value of ca. 0.25 atom per formula unit, whereas the Mn^{2+} content at the M2 site increases linearly with increasing x. This linear behavior indicates that large amounts of Mn^{2+} can occupy the M2 site, as has already been observed by Antenucci (1992), who inserted up to 50 atomic% Mn^{2+} at the M2 site of the alluaudite-like compounds, $Na_2Mn_2M(PO_4)_3$, where M is Fe^{3+}, In^{3+}, Cr^{3+}, or Al^{3+}. For x = 0.00, Figure 4 indicates the absence of Mn^{2+} at the M2 site of the alluaudite structure, thus confirming data previously published by Hatert et al. (2000).

Variation of the unit-cell parameters

The unit-cell parameters of the $NaMn(Fe_{1-x}In_x)_2(PO_4)_3$ alluaudite-like compounds given in Table 1 increase in a linear fashion with increasing x due to the replacement of Fe^{3+}

TABLE 3. Reliability factors for the Rietveld refinements of thealluaudite-like compounds, $NaMn(Fe_{1-x}In_x)_2(PO_4)_3$

x	0.25	0.50	0.75	1.00
R_p (%)	2.54	2.57	3.08	4.31
R_{wp} (%)	3.54	3.57	4.20	5.94
$R_{exp.}$ (%)	1.65	1.99	2.21	2.44
S	2.13	1.78	1.89	2.42
R_{Bragg} (%)	5.44	2.98	3.35	4.65

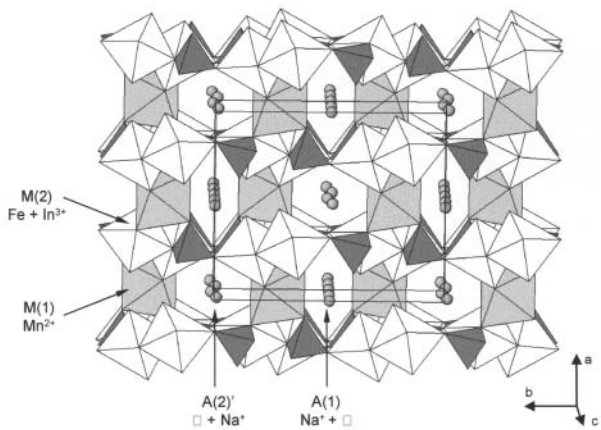

FIGURE 2. A projection of the crystal structure of $NaMnFeIn(PO_4)_3$. The PO_4 tetrahedra are densely shaded. The shaded M1 octahedra are occupied by Mn^{2+}, and the unshaded M2 octahedra are occupied by Fe and In^{3+}. The circles indicate Na^+ at the A1 and A2' crystallographic sites.

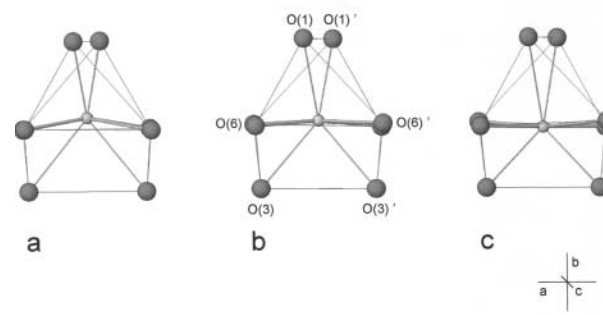

FIGURE 3. Morphology of the A2' crystallographic site in the $NaMn(Fe_{1-x}In_x)_2(PO_4)_3$ alluaudite-like compounds, for x values of 0.25 (**a**), 0.50 (**b**), and 0.75 (**c**).

TABLE 4. Positional (*x, y, z*), isotropic thermal (*B*) and site occupancy (*N*) parameters for the synthetic alluaudite-like compounds, $NaMn(Fe_{1-x}In_x)_2(PO_4)_3$

Site	Wyckoff	Atom	*x*	*y*	*z*	*B*(Å²)	N	*x*	*y*	*z*	*B*(Å²)	N
			$NaMnFe_{1.5}In_{0.5}(PO_4)_3$					$NaMnFeIn(PO_4)_3$				
A2'	4*e*	Na	0	–0.03(1)	1/4	1.0	0.033(4)	0	–0.011(5)	1/4	1.0	0.059(4)
A1	4*b*	Na	1/2	0	0	3.3(4)	0.500(7)	1/2	0	0	3.3(4)	0.490(6)
M1	4*e*	Mn	0	0.2650(3)	1/4	0.6(2)	0.426(4)	0	0.2631(2)	1/4	0.8(2)	0.390(4)
		In	0	0.2650(3)	1/4	0.6(2)	0.074	0	0.2631(2)	1/4	0.8(2)	0.110
M2	8*f*	Fe	0.2831(3)	0.6520(2)	0.3717(5)	0.8(1)	0.75	0.2831(2)	0.6504(1)	0.3731(4)	0.33(8)	0.5
		In	0.2831(3)	0.6520(2)	0.3717(5)	0.8(1)	0.218(8)	0.2831(2)	0.6504(1)	0.3731(4)	0.33(8)	0.413(8)
		Mn	0.2831(3)	0.6520(2)	0.3717(5)	0.8(1)	0.032	0.2831(2)	0.6504(1)	0.3731(4)	0.33(8)	0.087
P1	4*e*	P	0	–0.2825(5)	1/4	0.6(2)	0.5	0	–0.2886(5)	1/4	0.3(1)	0.5
P2	8*f*	P	0.2375(5)	–0.1086(4)	0.1331(9)	0.6(2)	1.0	0.2407(4)	–0.1099(4)	0.1306(8)	0.3(1)	1.0
O1	8*f*	O	0.4589(8)	0.7284(8)	0.529(2)	0.4(2)	1.0	0.4549(7)	0.7199(7)	0.534(1)	0.2(1)	1.0
O2	8*f*	O	0.0969(9)	0.6358(7)	0.234(1)	0.4(2)	1.0	0.0977(7)	0.6355(6)	0.242(1)	0.2(1)	1.0
O3	8*f*	O	0.3242(8)	0.6609(7)	0.106(2)	0.4(2)	1.0	0.3304(7)	0.6625(6)	0.104(1)	0.2(1)	1.0
O4	8*f*	O	0.1329(8)	0.3955(6)	0.327(1)	0.4(2)	1.0	0.1278(7)	0.3942(5)	0.324(1)	0.2(1)	1.0
O5	8*f*	O	0.2239(8)	0.8283(7)	0.315(2)	0.4(2)	1.0	0.2234(7)	0.8212(6)	0.312(1)	0.2(1)	1.0
O6	8*f*	O	0.3110(6)	0.5012(9)	0.371(1)	0.4(2)	1.0	0.3122(6)	0.4970(8)	0.370(1)	0.2(1)	1.0
			$NaMnFe_{0.5}In_{1.5}(PO_4)_3$					$NaMnIn_2(PO_4)_3$				
A2'	4*e*	Na	0	0.008(6)	1/4	1.0	0.052(4)	0	0.069(6)	1/4	1.0	0.059(6)
A1	4*b*	Na	1/2	0	0	3.7(4)	0.498(7)	1/2	0	0	3.4(5)	0.501(9)
M1	4*e*	Mn	0	0.2635(2)	1/4	1.0(2)	0.377(4)	0	0.2641(3)	1/4	1.1(2)	0.384(4)
		In	0	0.2635(2)	1/4	1.0(2)	0.123	0	0.2641(3)	1/4	1.1(2)	0.116
M2	8*f*	Fe	0.2844(2)	0.6497(1)	0.3740(3)	0.52(7)	0.25	–	–	–	–	–
		In	0.2844(2)	0.6497(1)	0.3740(3)	0.52(7)	0.64(1)	0.2856(2)	0.6488(1)	0.3759(3)	0.17(8)	0.85(1)
		Mn	0.2844(2)	0.6497(1)	0.3740(3)	0.52(7)	0.11	0.2856(2)	0.6488(1)	0.3759(3)	0.17(8)	0.15
P1	4*e*	P	0	–0.2898(5)	1/4	0.2(1)	0.5	0	–0.2935(6)	1/4	0.3(1)	0.5
P2	8*f*	P	0.2407(4)	–0.1116(4)	0.1329(9)	0.2(1)	1.0	0.2394(5)	–0.1131(5)	0.129(1)	0.3(1)	1.0
O1	8*f*	O	0.4560(8)	0.7198(7)	0.536(1)	0.1(2)	1.0	0.458(1)	0.7225(9)	0.543(2)	1.0	1.0
O2	8*f*	O	0.0972(7)	0.6335(7)	0.242(1)	0.1(2)	1.0	0.1005(9)	0.6343(9)	0.251(2)	1.0	1.0
O3	8*f*	O	0.3325(7)	0.6625(7)	0.105(1)	0.1(2)	1.0	0.3366(9)	0.663(1)	0.109(2)	1.0	1.0
O4	8*f*	O	0.1291(8)	0.3934(5)	0.328(1)	0.1(2)	1.0	0.128(1)	0.3932(7)	0.330(2)	1.0	1.0
O5	8*f*	O	0.2252(7)	0.8198(6)	0.311(1)	0.1(2)	1.0	0.2258(9)	0.8181(8)	0.310(2)	1.0	1.0
O6	8*f*	O	0.3130(6)	0.4937(8)	0.369(1)	0.1(2)	1.0	0.3121(9)	0.496(1)	0.365(2)	1.0	1.0

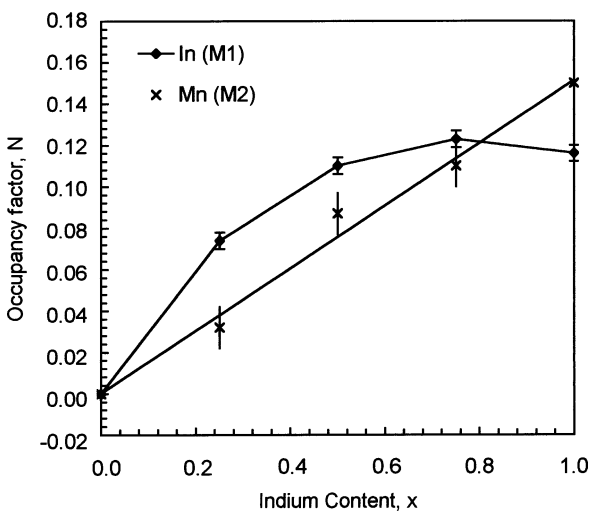

FIGURE 4. The compositional dependence of the site occupancies in $NaMn(Fe_{1-x}In_x)_2(PO_4)_3$.

by In^{3+} at the M2 crystallographic site. This increase in the unit-cell parameters (Fig. 5) correlates with the variation of bond distances induced by the incorporation of indium into the alluaudite structure. The differences between the bond distances of $NaMnFe_2(PO_4)_3$ and $NaMnIn_2(PO_4)_3$, presented in Table 5, clearly indicate that significant variations in the bond distances occur for the A1 and M2 crystallographic sites. Indeed, for the M2 crystallographic site, the nearly isotropic increase in the bond distances does not result in an isotropic increase of the unit-cell parameters (Fig. 5). This behavior is probably related to the orientation of the M2-O5 and M2-O6 bonds, which are parallel to the **b** axis. In contrast, no bonds are parallel to the **a** and **c** axes (Fig. 6). Consequently, the increase in the *b* unit-cell parameter is more important that the increase in the *a* and *c* parameters (Fig. 5).

As shown in Figure 7, the significant increase in the β angle correlates with the M1-M2 distances given in Table 5, a correlation that can be qualitatively understood as follows. The increasing M1-M2 distance indicates an elongation of the octahedral chains of the alluaudite structure, resulting in an increased β angle (Fig. 8). The variations in the A2'-O bond distances are related to the displacement of the Na^+ atoms at this crystallographic site (Fig. 3). Consequently, these variations of bond distances do not affect the unit-cell parameters.

Infrared spectroscopy

The infrared spectra of $NaMn(Fe_{1-x}In_x)_2(PO_4)_3$, shown in Figure 9, are typical of an orthophosphate structure (Rulmont et al. 1991). Qualitatively, sharp bands are observed for x = 0.00 and 1.00, whereas broader bands are observed for the compounds with x = 0.25, 0.50, and 0.75. This feature can probably be related to the disordered distribution of Fe^{3+} and In^{3+} at the M2 crystallographic site for the intermediate compounds.

Because the infrared spectra of alluaudites exhibit a complexity that is related both to the low symmetry and to the large unit cell of the alluaudite structure (Antenucci et al.

TABLE 5. Selected interatomic distances (Å) and angles (°) for the synthetic alluaudite-like compounds, $NaMn(Fe_{1-x}In_x)_2(PO_4)_3$

x	0.00 (*)	0.25	0.50	0.75	1.00	Difference
A2'-O6 × 2	2.526(2)	2.57(2)	2.562(7)	2.563(7)	2.73(3)	0.20
A2'-O6 × 2	2.693(2)	2.73(2)	2.699(5)	2.711(7)	2.87(3)	0.18
A2'-O1 × 2	2.868(6)	2.8(1)	2.95(5)	3.19(7)	2.96(6)	0.09
A2'-O3 × 2	2.888(5)	3.07(9)	2.90(5)	2.72(6)	2.19(5)	–0.70
Mean	2.74	2.79	2.78	2.80	2.69	–0.05
A1-O2 × 2	2.320(1)	2.260(8)	2.299(7)	2.291(8)	2.35(1)	0.03
A1-O4 × 2	2.333(1)	2.434(8)	2.425(7)	2.461(7)	2.48(1)	0.15
A1-O4 × 2	2.581(1)	2.653(7)	2.647(6)	2.668(7)	2.666(8)	0.09
A1-O2 × 2	2.979(1)	2.984(8)	2.971(7)	2.976(7)	2.989(9)	0.01
Mean	2.55	2.58	2.59	2.60	2.62	0.07
M1-O1 × 2	2.191(1)	2.104(8)	2.197(7)	2.220(8)	2.253(9)	0.06
M1-O4 × 2	2.175(1)	2.208(8)	2.191(6)	2.203(7)	2.199(9)	0.02
M1-O3 × 2	2.246(1)	2.335(8)	2.266(7)	2.264(7)	2.24(1)	–0.01
Mean	2.20	2.22	2.22	2.23	2.23	0.03
M2-O6	1.925(1)	1.94(1)	1.99(1)	2.04(1)	2.01(1)	0.09
M2-O3	2.029(1)	1.973(8)	2.056(7)	2.075(7)	2.103(9)	0.07
M2-O2	1.991(1)	2.053(8)	2.052(6)	2.085(6)	2.071(7)	0.08
M2-O5	2.053(1)	2.064(9)	2.104(8)	2.136(8)	2.17(1)	0.12
M2-O1	2.057(1)	2.160(8)	2.095(7)	2.108(7)	2.152(9)	0.10
M2-O5	2.220(1)	2.322(9)	2.276(8)	2.283(8)	2.29(1)	0.07
Mean	2.05	2.09	2.10	2.12	2.13	0.08
M1-M2	3.335(1)	3.347(3)	3.374(2)	3.396(2)	3.420(2)	
P1-O1 × 2	1.545(1)	1.46(1)	1.541(9)	1.548(9)	1.54(1)	–0.01
P1-O2 × 2	1.541(1)	1.595(9)	1.547(7)	1.561(8)	1.55(1)	+0.01
Mean	1.54	1.53	1.54	1.55	1.55	0.00
P2-O4	1.525(1)	1.476(7)	1.496(6)	1.502(7)	1.537(8)	0.01
P2-O5	1.557(1)	1.48(1)	1.549(9)	1.532(9)	1.54(1)	–0.02
P2-O6	1.530(1)	1.50(1)	1.51(1)	1.50(1)	1.55(1)	0.02
P2-O3	1.553(1)	1.55(1)	1.548(9)	1.57(1)	1.57(1)	0.02
Mean	1.54	1.50	1.53	1.53	1.55	0.01
O2-P1-O2	104.8(1)	99.3(5)	102.6(5)	101.7(5)	105.6(7)	
O1-P1-O2 × 2	108.54(7)	101.6(4)	108.2(4)	108.5(4)	109.3(5)	
O1-P1-O2 × 2	112.31(7)	113.8(4)	113.5(4)	114.6(4)	113.2(5)	
O1-P1-O1	110.25(9)	124.3(7)	110.7(6)	109.0(6)	106.4(8)	
Mean	109.5	109.1	109.5	109.5	109.5	
O4-P2-O3	110.62(8)	103.0(5)	108.5(4)	107.8(4)	109.3(5)	
O4-P2-O5	108.68(7)	109.9(5)	110.0(4)	111.0(5)	110.6(6)	
O5-P2-O6	109.96(7)	110.0(5)	108.8(4)	109.2(4)	109.1(6)	
O4-P2-O6	111.23(7)	110.3(5)	112.8(4)	113.0(4)	111.1(6)	
O6-P2-O3	108.70(7)	110.7(5)	109.2(4)	107.8(5)	108.6(6)	
O5-P2-O3	107.58(7)	112.8(6)	107.5(5)	107.9(5)	108.1(6)	
Mean	109.5	109.5	109.5	109.5	109.5	

* Single-crystal structure refinement data from Hatert et al. (2000).

1993), it is difficult to assign all the individual absorption bands. Nevertheless, the similarity of the $NaMn(Fe_{1-x}In_x)_2(PO_4)_3$ spectra with that of $NaCdIn_2(PO_4)_3$ permits the assignments proposed by Antenucci et al. (1993) to be used for $NaMn(Fe_{1-x}In_x)_2(PO_4)_3$. According to these authors, the stretching vibrational modes of the PO_4 tetrahedra occur in the 1200–850 cm^{-1} region, whereas the PO_4 bending vibrational modes occur between ca. 400 and 650 cm^{-1}. Starting from these hypotheses, a more detailed assignment of the absorption bands is presented in Table 6.

According to the fundamental vibrational frequencies of the PO_4 tetrahedron given by Farmer (1974), the absorption bands between 939 and 1111 cm^{-1} can be assigned to ν_3, the antisymmetric stretching modes of the PO_4 anions, whereas the bands between 517 and 599 cm^{-1} can be assigned to ν_4, their bending mode. The weak band at 902 cm^{-1} in the spectrum of $NaMnIn_2(PO_4)_3$ probably corresponds to ν_1, the symmetric stretching mode of the PO_4 tetrahedron.

When the indium-content of the $NaMn(Fe_{1-x}In_x)_2(PO_4)_3$ solid solution increases, the infrared spectra show the emergence of weak absorption bands that can be attributed to In^{3+}-O vibrations. In the spectrum of $NaMnIn_2(PO_4)_3$, these bands are localized at 229, 308, 345, 488, 613, and 634 cm^{-1} (Table 6). A study by White and Keramidas (1972) of the infrared spectra of several oxides has established a correlation between the highest frequency band in the spectra and the M^{3+}-O bond distance. According to this correlation, the highest frequency band for the In^{3+}-O vibrational mode at 634 cm^{-1} corresponds to an In^{3+}-O distance of 2.12 Å, a value that is close to the mean bond length of 2.13 Å (Table 5).

The replacement of Fe^{3+} by In^{3+} also leads to the disappearance of weak bands at 249, 327, and 466 cm^{-1} in the spectrum of $NaMnFe_2(PO_4)_3$, bands that can reasonably be assigned to the Fe^{3+}-O vibrations. The absorption bands at ca. 414 and

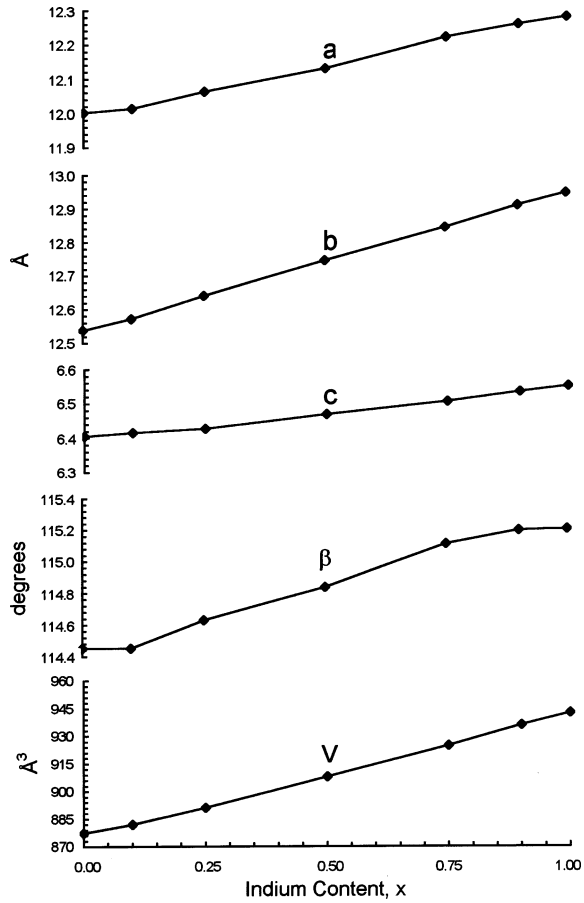

FIGURE 5. The compositional dependence of the unit-cell parameters of $NaMn(Fe_{1-x}In_x)_2(PO_4)_3$. The error bars are smaller than the data points.

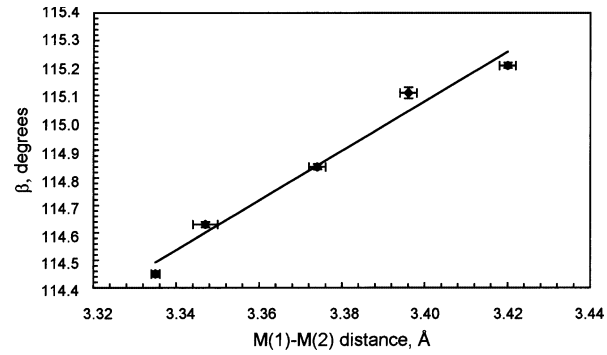

FIGURE 7. The correlation between the b angle and the M1-M2 distance in the alluaudite-like compounds, $NaMn(Fe_{1-x}In_x)_2(PO_4)_3$.

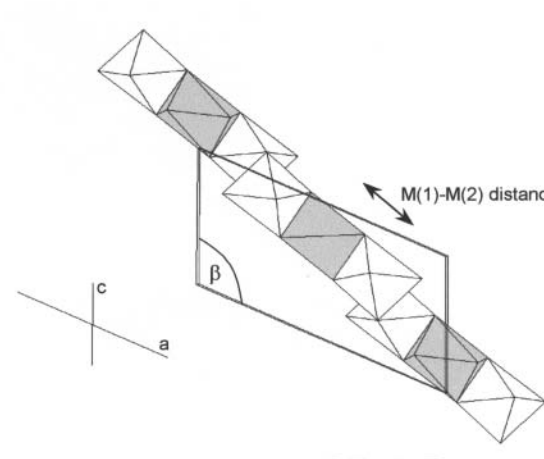

FIGURE 8. A projection of the octahedral M chains of the alluaudite structure showing the relationship between the M1-M2 distance and the b angle in the alluaudite-like compounds, $NaMn(Fe_{1-x}In_x)_2(PO_4)_3$. The M1 octahedra are shaded.

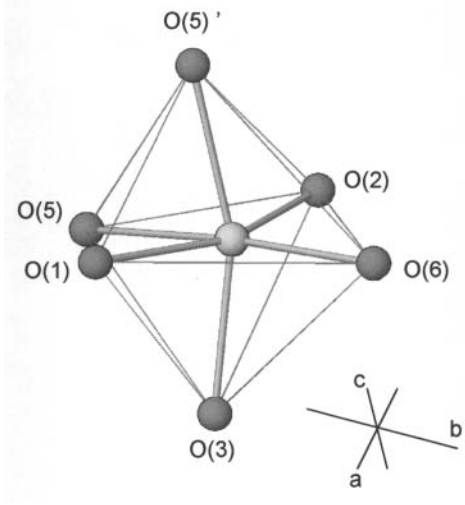

FIGURE 6. Morphology of the M2 crystallographic site in the alluaudite-like compound, $NaMnFeIn(PO_4)_3$.

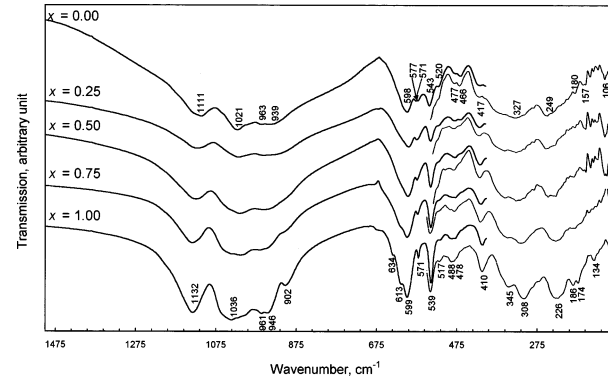

FIGURE 9. The infrared spectra of the $NaMn(Fe_{1-x}In_x)_2(PO_4)_3$ alluaudite-like compounds.

478 cm^{-1} are observed in the spectra for x = 0.00 to 1.00, suggesting their possible assignment to Mn^{2+}-O vibrational modes or to PO_4 bending modes.

^{57}Fe Mössbauer spectroscopy

The 90 K Mössbauer spectra of $NaMn(Fe_{1-x}In_x)_2(PO_4)_3$, with x = 0.00, 0.10, 0.25, 0.75, 0.90, and 0.99 are shown in Figure 10 and the spectra of $NaMnFeIn(PO_4)_3$, obtained at five different temperatures, are shown in Figure 11. The general appearance of these spectra indicate that they should be fit with at least two doublets, one assigned to Fe^{2+} and having a large isomer shift and quadrupole splitting, and a second assigned to Fe^{3+} and having a small isomer shift and quadrupole splitting. However, the poor fits and the broad linewidths of ca. 0.45 mm/s obtained with such preliminary fits suggested that a reasonable spectral fit requires at least two Fe^{2+} doublets and two Fe^{3+} doublets.

A model for the Mössbauer spectral analysis has been developed (Hermann et al. 2001) on the basis of the alluaudite crystal structure (Hatert et al. 2000). In this model, four different next-nearest neighbor iron environments are possible (Fig. 12), if one assumes both a random distribution of Fe^{2+},

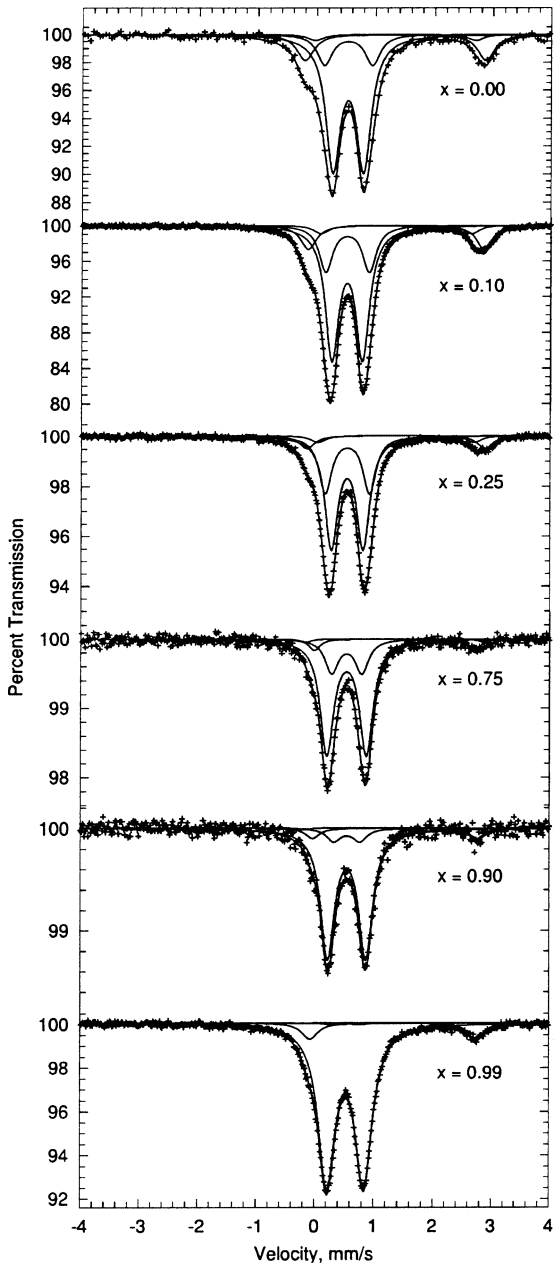

FIGURE 10. The Mössbauer spectra of $NaMn(Fe_{1-x}In_x)_2(PO_4)_3$ obtained at 90 K.

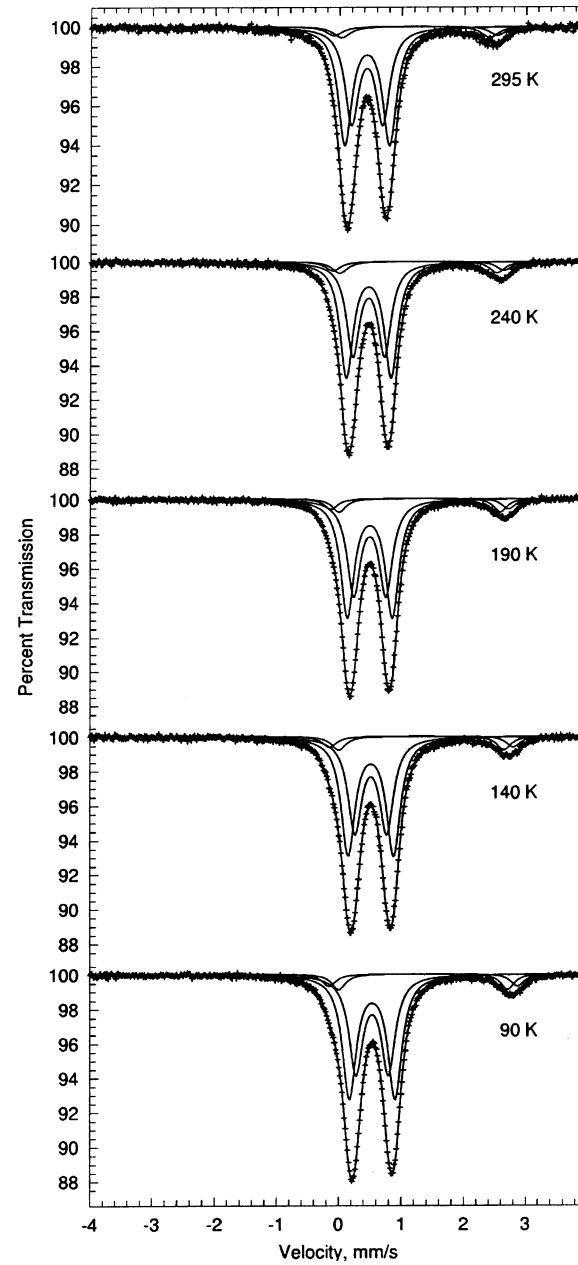

FIGURE 11. The Mössbauer spectra of $NaMnFeIn(PO_4)_3$ obtained at the indicated temperatures.

Fe^{3+}, and In^{3+} at the M2 sites and that the Fe^{2+} and In^{3+} ions are equivalent in their perturbation of the spectral hyperfine parameters. The latter assumption is justified because the Fe^{2+} and In^{3+} cations have similar six-coordinate ionic radii of 0.780 and 0.800 Å (Shannon 1976), respectively, and because it has been shown that the different cation charges do not significantly influence the hyperfine parameters (Hermann et al. 2001). Thus, if g and $(1 - g)$ are the Fe^{2+} and Fe^{3+} fractions of the total iron content, respectively, and if x is the In^{3+} content, the probabilities given in Figure 12 for the four different iron environments of a given M2 site are obtained. Given these assumptions, the Mössbauer spectra should exhibit two Fe^{2+} and two Fe^{3+} quadrupole doublets. A fit with these assumptions would require 15 adjustable parameters, but preliminary fits indicated that the isomer shifts and linewidths of the two Fe^{2+} and two Fe^{3+} doublets were identical within experimental error. Thus, the final fits involved the adjustment of only 11 parameters, one Fe^{2+} fraction, g, two isomer shifts, δ, four quadrupole splittings, ΔE_Q, and two linewidths, Γ, as well as the total spectral area and spectral baseline. The value of x was fixed to its stoichiometric value. The resulting fits are excellent as is shown in Figures 10 and 11; the best-fit hyperfine parameters for the four environments are given in Table 7.

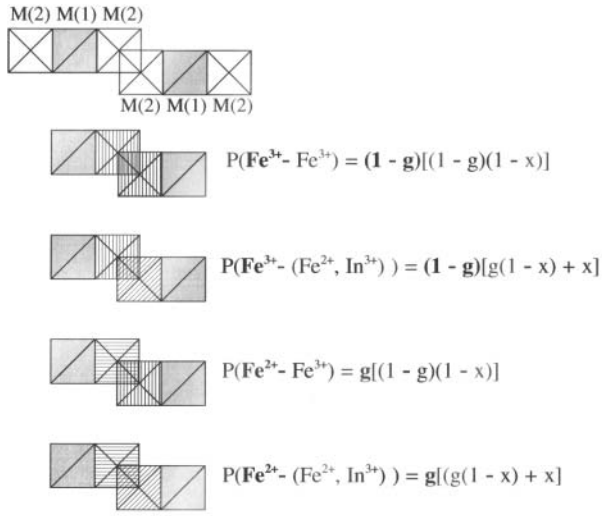

FIGURE 12. The four different configurations of next-nearest neighbor M2 sites occupied by Fe^{3+}, Fe^{2+}, and In^{3+} and the probabilities as obtained for the iron ion in bold face type. The vertical lines represent the M2 sites occupied by Fe^{3+}, the horizontal lines by Fe^{2+}, and the obliques by Fe^{2+} or In^{3+}.

TABLE 6. Assignments of the infrared frequencies for the alluaudite-like compounds, $NaMn(Fe_{1-x}In_x)_2(PO_4)_3$

0.00	0.25	0.50	0.75	1.00	Assignment
1111					
	1123	1123			
			1133	1132	
			1135	1136	ν_3 PO_4
1021	1019	1014	1013		
963	957		965	961	
		951	951	946	
939					
			908	902	ν_1 PO_4
				634	In^{3+}-O
			614	613	In^{3+}-O
598	594	596	599	599	
577	575	574	572	571	ν_4 PO_4
571					
543	540	540	540	539	
520	520	518	517	517	
				488	In^{3+}-O
477	479	478	478	478	Mn^{2+}-O or PO_4 bending?
466	467				Fe^{3+}-O
417	418	416	414	410	Mn^{2+}-O or PO_4 bending?
	354	353	348	345	In^{3+}-O
327	326	326			Fe^{3+}-O
		318	315	308	In^{3+}-O
249	248	247			Fe^{3+}-O
	230	229	228	229	In^{3+}-O

The fraction, g, of Fe^{2+} obtained from Mössbauer spectroscopy, which ranges from 7.5 to 19.1 atomic percent of the total iron content at 90 K, is substantially larger than that obtained by chemical analysis that gives values ranging from 0.0 to 11.8 percent. However, both the chemical analysis and Mössbauer spectroscopy indicate that the Fe^{2+} content decreases with increasing x. This behavior is discussed in detail below. As is well known (De Grave and Van Alboom 1991), the Fe^{2+} recoil-free fraction decreases more with increasing temperature than does that of Fe^{3+}, a difference that explains the slight decrease in g observed with increasing temperature. The following discussion will use the values of g obtained at 90 K, a temperature at which the Fe^{2+} and Fe^{3+} recoil free fractions can be assumed to be equal (De Grave and Van Alboom 1991).

In agreement with the second order Doppler shift, both the Fe^{2+} and Fe^{3+} isomer shifts decrease with increasing temperature, as is illustrated in Figure 13 for $NaMnFeIn(PO_4)_3$. A similar linear behavior has been observed for all the other compounds under study herein and the zero temperature intercepts, $\delta(0)$, and the slopes, $d\delta/dT$, are given in Table 8.

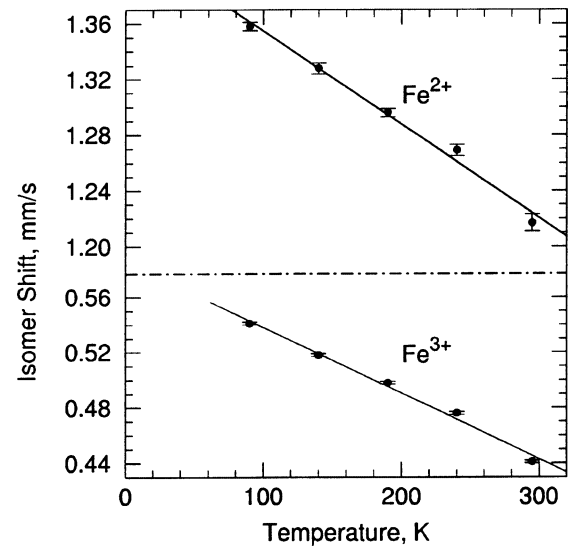

FIGURE 13. The temperature dependence of the isomer shifts of $NaMnFeIn(PO_4)_3$.

TABLE 7. Mössbauer spectral parameters for $NaMn(Fe_{1-x}In_x)_2(PO_4)_3$

		A		Fe^{3+} (mm/s)				Fe^{2+} (mm/s)			
x	*T* (K)	[(%ε)(mm/s)]/(mg/cm²)	g (%)	δ*	$\Delta E_{Q,3-3}$	$\Delta E_{Q,3-2}$	Γ	δ*	$\Delta E_{Q,2-3}$	$\Delta E_{Q,2-2}$	Γ
0.00	295	–0.828(2)	17.8(4)	0.428(1)	0.520(1)	0.77(1)	0.309(2)	1.253(5)	2.71(1)	2.09(7)	0.43(1)
	240	–0.853(2)	18.2(4)	0.444(1)	0.521(1)	0.77(1)	0.298(2)	1.264(4)	2.78(1)	2.19(7)	0.42(1)
	190	–0.887(3)	18.3(4)	0.470(1)	0.522(2)	0.77(1)	0.309(2)	1.301(5)	2.87(1)	2.32(7)	0.42(2)
	140	–0.918(3)	19.3(4)	0.493(1)	0.524(2)	0.77(1)	0.301(2)	1.325(4)	2.96(1)	2.44(6)	0.41(1)
	90	–0.943(2)	19.1(4)	0.513(1)	0.525(1)	0.77(1)	0.294(2)	1.341(4)	3.04(1)	2.48(5)	0.38(1)
0.10	295	–1.225(3)	16.6(3)	0.439(1)	0.518(2)	0.733(6)	0.289(2)	1.259(3)	2.637(7)	2.06(3)	0.35(1)
	225	–1.277(3)	16.7(3)	0.468(1)	0.518(2)	0.739(6)	0.287(2)	1.282(4)	2.765(8)	2.31(3)	0.36(1)
	155	–1.355(4)	17.5(3)	0.505(1)	0.520(2)	0.743(7)	0.289(2)	1.328(4)	2.907(8)	2.40(3)	0.33(1)
	90	–1.415(3)	18.2(2)	0.529(1)	0.519(1)	0.740(5)	0.281(2)	1.355(3)	2.990(6)	2.56(2)	0.33(1)
0.25	295	–0.861(3)	11.7(4)	0.438(1)	0.538(2)	0.734(5)	0.265(3)	1.259(5)	2.65(1)	2.02(3)	0.29(2)
	240	–0.935(4)	12.2(4)	0.470(1)	0.536(2)	0.748(4)	0.268(3)	1.306(6)	2.77(1)	2.11(3)	0.31(2)
	190	–0.983(5)	12.5(4)	0.496(1)	0.528(2)	0.748(4)	0.269(2)	1.319(6)	2.85(2)	2.51(4)	0.35(3)
	140	–1.019(4)	12.5(3)	0.521(1)	0.535(2)	0.752(3)	0.266(2)	1.346(5)	2.93(1)	2.52(2)	0.32(2)
	90	–1.069(2)	12.6(4)	0.539(1)	0.539(2)	0.752(4)	0.268(2)	1.366(5)	3.03(1)	2.65(3)	0.31(2)
0.50	295	–1.406(6)	10.7(5)	0.441(1)	0.498(3)	0.718(2)	0.269(3)	1.217(7)	2.66(4)	2.38(3)	0.33(3)
	240	–1.514(6)	11.1(4)	0.476(1)	0.508(3)	0.717(2)	0.257(2)	1.269(4)	2.75(3)	2.52(2)	0.30(2)
	190	–1.570(5)	11.0(3)	0.498(1)	0.514(2)	0.719(2)	0.261(2)	1.296(3)	2.85(2)	2.59(1)	0.27(2)
	140	–1.632(5)	11.2(3)	0.518(1)	0.507(3)	0.726(2)	0.270(2)	1.328(4)	2.95(2)	2.65(1)	0.28(2)
	90	–1.697(5)	11.8(2)	0.541(1)	0.517(2)	0.729(2)	0.268(2)	1.358(3)	3.02(1)	2.71(1)	0.28(1)
0.75	295	–0.809(6)	11.6(9)	0.445(1)	0.48(2)	0.661(5)	0.286(6)	1.19‡	2.73‡	2.38‡	0.38(5)
	240	–0.828(6)	9.7(6)	0.478(1)	0.50(2)	0.664(4)	0.280(5)	1.28(1)	2.85(9)	2.53(2)	0.28(4)
	190	–0.867(6)	9.6(6)	0.498(1)	0.51(2)	0.662(5)	0.277(5)	1.32(1)	2.92(7)	2.62(2)	0.24(3)
	140	–0.891(7)	8.3(9)	0.519(1)	0.49(2)	0.677(4)	0.270(6)	1.32(1)	2.9(2)	2.66(3)	0.27(6)
	90	–0.930(9)	8.4(8)	0.540(1)	0.51(2)	0.670(6)	0.280(6)	1.36(1)	3.02‡	2.73(2)	0.24(4)
0.90	295	–1.80(2)	7.4(5)	0.45(1)	0.384(2)	0.64(7)	0.304(5)	1.19‡	2.73‡	2.41‡	0.3‡
	240	–1.90(3)	5.4(7)	0.48(1)	0.489(3)	0.64(10)	0.30(1)	1.28‡	2.85‡	2.53‡	0.3‡
	190	–2.06(3)	6.3(6)	0.50(1)	0.475(2)	0.64(10)	0.30(1)	1.31‡	2.85‡	2.65‡	0.3‡
	140	–2.09(2)	6.7(6)	0.53(1)	0.469(2)	0.65(10)	0.29(1)	1.35(3)	2.88‡	2.75(3)	0.3‡
	90	–2.67(2)	7.5(6)	0.546(7)	0.441(2)	0.65(6)	0.289(7)	1.36(2)	3.02‡	2.79(4)	0.3‡
0.99	295	–1.219(5) †	8.5(4)	0.444(1)	–[d]	0.609(1)	0.355(2)	1.206(7)	–[d]	2.51(2)	0.35(3)
	240	–1.254(5) †	8.2(4)	0.461(1)	–[d]	0.614(2)	0.355(3)	1.224(7)	–[d]	2.55(1)	0.33(3)
	190	–1.313(5) †	8.9(3)	0.486(1)	–[d]	0.618(1)	0.348(2)	1.278(6)	–[d]	2.64(1)	0.35(2)
	140	–1.378(7) †	9.3(4)	0.509(1)	–[d]	0.624(3)	0.352(4)	1.308(7)	–[d]	2.72(2)	0.36(4)
	90	–1.432(7) †	9.2(4)	0.527(1)	–[d]	0.628(4)	0.348(4)	1.334(6)	–[d]	2.82(2)	0.34(3)

* Relative to α-iron foil.
† 50[(%ε)(mm/s)]/(mg/cm²) to take into account the enriched 57Fe content.
‡ Constrained value. **{{auth: what does footnote d stand for? please define or we'll delete. If defined, note that we'll use § not d.}}**

TABLE 8. Parameters obtained from the temperature dependence of the Mössbauer spectra of $NaMn(Fe_{1-x}In_x)_2(PO_4)_3$

x	0.00	0.10	0.25	0.50	0.75	0.90	0.99
$10^4 \leftrightarrow$ dδ/d*T* Fe^{2+} [(mm/s)/K]	–4.6(2)	–4.9(5)	–5.0(5)	–5.1(5)	–7.2(2.0)	–	–6.6(6)
$10^4 \leftrightarrow$ dδ/d*T* Fe^{3+} [(mm/s)/K]	–4.3(5)	–4.5(2)	–5.0(2)	–4.9(4)	–4.5(2)	–4.8(2)	–4.2(2)
δ(0) Fe^{2+} (mm/s)	1.385(9)	1.399(9)	1.41(1)	1.40(1)	1.43(3)	–	1.40(1)
δ(0) Fe^{3+} (mm/s)	0.552(4)	0.571(4)	0.588(5)	0.588(7)	0.583(4)	0.591(3)	0.566(3)
$10^4 \leftrightarrow$ d(ln Area)/d*T* (K^{-1})	–6.4(4)	–7.2(3)	–10.2(8)	–9.1(8)	–6.9(4)	–10(2)	–8.2(5)
M_{eff} Fe^{2+} (g/mol)	90(9)	85(9)	84(8)	82(8)	58(16)	–	63(6)
M_{eff} Fe^{3+} (g/mol)	96(4)	93(4)	84(3)	84(7)	92(4)	87(4)	99(5)
θ_M Fe^{2+} (K)	369(21)	355(20)	301(20)	324(20)	440(65)	–	390(20)
θ_M Fe^{3+} (K)	357(13)	340(10)	301(13)	319(20)	351(13)	294(30)	310(12)
Δ_{2-3} (cm^{-1})	542(30)	508(30)	512(24)	514(24)	567(50)	–	–
$\Delta E_{Q,2-3}(0)$ (mm/s)	3.05*	3.05*	3.05*	3.05*	3.05*	–	–
Δ_{2-2} (cm^{-1})	495(20)	433(20)	381(18)	459(22)	528(16)	–	513(34)
$\Delta E_{Q,2-2}(0)$ (mm/s)	2.46(2)	2.6*	2.7*	2.75*	2.75*	–	2.85*

* Parameter constrained to the value given.

From these slopes and that of the logarithm of the absorption area, d(ln Area)/d*T*, the effective vibrating masses and Mössbauer lattice temperatures, θ_M, have been calculated (Herber 1984) and are also given in Table 8. Because the Fe^{3+} Mössbauer lattice temperatures are between 294 and 440 K, the linear approximation used for the temperature dependence of the isomer shift between 90 and 295 K is rather poor (Long et al. 2000) and the relatively large effective vibrating masses of ca. 90 g/mol are probably overestimated. The reasonable temperature dependence of the isomer shifts does, however, serve to validate the model used to fit the spectra. The observed 294 to 440 K range of Mössbauer lattice temperatures are within the 288 to 460 K range typically observed for Fe^{3+} in the octahedral sites of the spinel structure (Vandenberghe and De Grave 1989). The Fe^{2+} Mössbauer lattice temperatures are systematically larger than those obtained for Fe^{3+}, probably because the larger Fe^{2+} cation is more tightly bound within the M2 site, a site that is normally occupied by the smaller Fe^{3+} cation.

As expected, within experimental error, the high-spin Fe^{3+} quadrupole splittings, $\Delta E_{Q,3-3}$ and $\Delta E_{Q,3-2}$, are independent of temperature. In contrast, but as expected, the high-spin Fe^{2+} quadrupole splittings, $\Delta E_{Q,2-2}$ and $\Delta E_{Q,2-3}$, increase substantially upon cooling (Fig. 14). The temperature dependence of

the Fe^{2+} quadrupole splitting, ΔE_Q, in a distorted environment may be calculated (Ingalls 1964) from the expression $\Delta E_Q = \Delta E_Q(0) \leftrightarrow \tanh(\Delta/(2kT))$, where $\Delta E_Q(0)$ is the quadrupole splitting at 0 K and Δ is the low-symmetry crystal field splitting of the octahedral Fe^{2+} orbital triplet ground state. The solid lines shown in Figure 14 correspond to the best fits of the quadrupole splittings with the model and the best-fit parameters are given in Table 8. A splitting of ca. 500 cm^{-1} is rather normal for a distorted octahedral environment (Hartmann-Boutron and Imbert 1968). The failure of the Ingalls' model to more adequately fit the Fe^{2+}-Fe^{3+} quadrupole splittings (Fig. 14) is an indication that the low-symmetry components of the octahedral crystal field are changing with temperature, changes that are not considered by the Ingalls' model. Indeed, such changes are expected in alluaudite-like compounds that have a non-compact crystal structure.

DISCUSSION AND CONCLUSIONS

The synthesis of the $NaMn(Fe_{1-x}In_x)_2(PO_4)_3$ solid solution confirms that alluaudite-like phosphates can easily accept In^{3+} as a trivalent cation, an observation that is in good agreement with the synthesis of $NaCdIn_2(PO_4)_3$ (Antenucci et al. 1993) and $Na_3In_2(PO_4)_3$ (Lii and Ye 1997). X-ray Rietveld refinements indicate a partially disordered distribution between Mn^{2+} and In^{3+} at the M1 and M2 sites of $NaMnIn_2(PO_4)_3$, whereas a non-disordered distribution of Cd^{2+} and In^{3+} at these crystallographic sites has been observed in $NaCdIn_2(PO_4)_3$ (Antenucci et al. 1993; Hatert et al. 2001). This difference is probably due to the similar ionic radii of Mn^{2+} and In^{3+}, radii that are 0.830 and 0.800 Å, respectively, whereas the ionic radius of Cd^{2+}, which is 0.95 Å, is significantly larger (Shannon 1976).

The compositional dependence of the Fe^{2+} content, obtained from the Mössbauer spectral analysis, is shown in Figure 15. The decrease in the Fe^{2+} content with increasing x can be qualitatively understood as follows. For steric reasons, the M2 crystallographic site cannot be completely filled with Fe^{3+}, and, as a consequence, small amounts of larger cations, such as Fe^{2+} or Mn^{2+}, are generally observed at this site in natural and synthetic alluaudites (Moore 1971; Moore and Ito 1979; Hatert et al. 2000; Hermann et al. 2001). Because Fe^{2+} and In^{3+} have similar radii of 0.780 and 0.800 Å, respectively, values that are larger than the Fe^{3+} radius of 0.645 Å (Shannon 1976), the replacement of Fe^{3+} by In^{3+} increases the mean ionic radius of the cations found at the M2 site. Consequently, the M2 site no longer needs to stabilize a small amount of Fe^{2+}. Hence, as the number of In^{3+} cations increases, the number of Fe^{2+} cations decreases.

The compositional dependence of the isomer shifts (Fig. 16) shows an increase of 0.03 mm/s of both the Fe^{3+} and Fe^{2+} isomer shifts from x = 0.00 to 0.25 and no significant variation for x above 0.25. This behavior is somewhat surprising in view of the linear compositional dependence of the unit-cell volume shown in Figure 5. The interpretation of the compositional dependence of the isomer shifts requires a finer

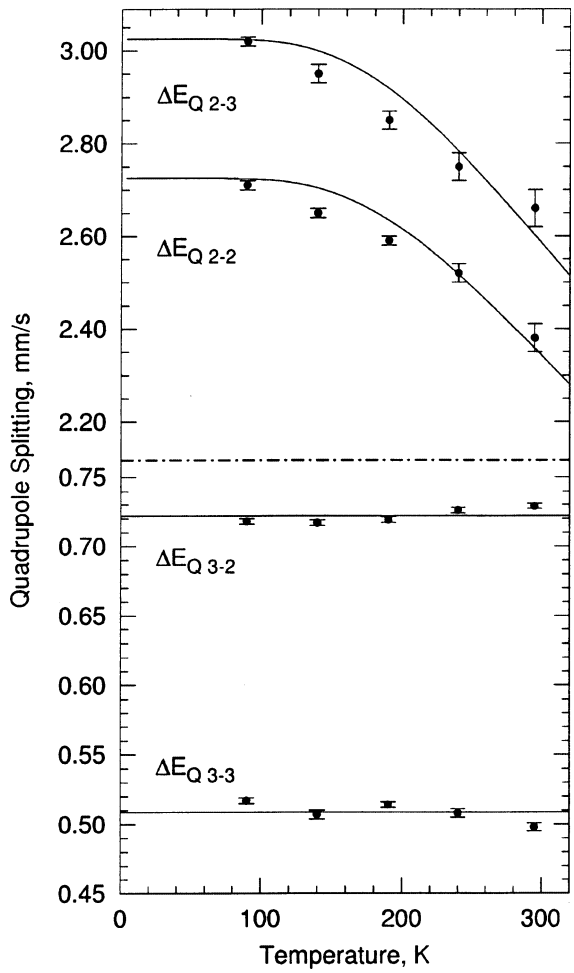

FIGURE 14. The temperature dependence of the quadrupole splittings of $NaMnFeIn(PO_4)_3$.

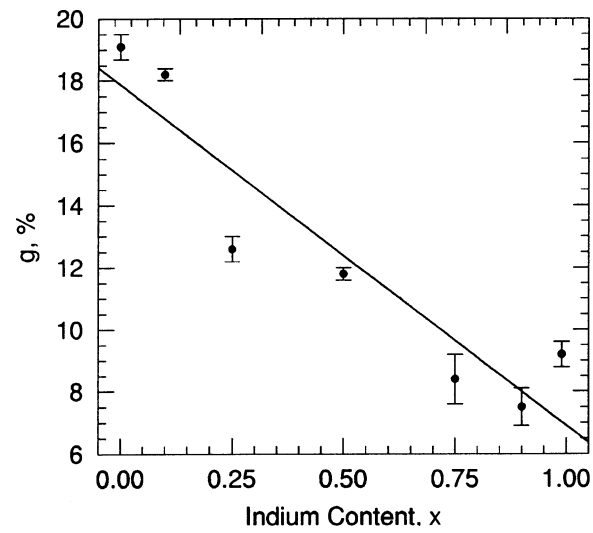

FIGURE 15. The compositional dependence of the Fe^{2+} content in $NaMn(Fe_{1-x}In_x)_2(PO_4)_3$.

analysis of the steric effect on the isomer shift. We will restrict our discussion to the Fe^{3+} isomer shift, because the Fe^{3+} doublets are the main components of the spectra. The relationship between the Fe^{3+} isomer shift in $NaMn(Fe_{1-x}In_x)_2(PO_4)_3$ (solid squares), and the mean Fe^{3+}-O distance from Table 5, is shown in Figure 17, where the open squares represent the data for $NaFe_{3.67}(PO_4)_3$ (Korzenski et al. 1998), $Na_{0.5}Li_{0.5}MnFe_2(PO_4)_3$ (Hermann et al. 2001), and $Ag_2Mn_2Fe(PO_4)_3$ (Chouaibi et al. 2001). The satisfactory linear fit, with R = 89%, indicates an increase in isomer shift of 0.23 (mm/s)/Å with the mean Fe^{3+}-O distance and hence the iron site volume, as x increases in $NaMn(Fe_{1-x}In_x)_2(PO_4)_3$. A similar linear dependence has been previously observed for Fe^{2+} in various phosphate minerals (Shinno and Li 1998).

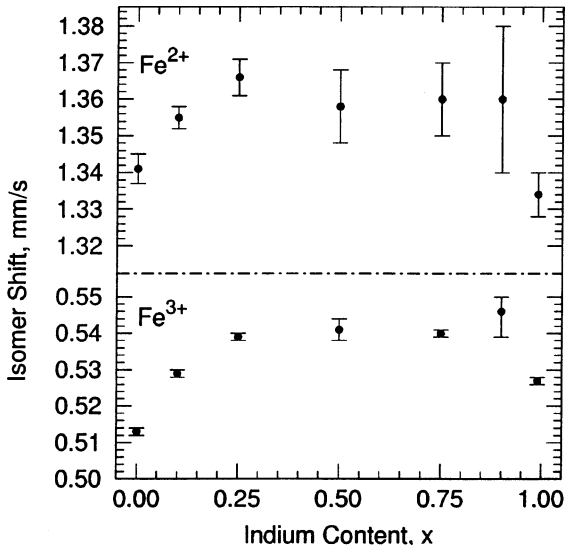

FIGURE 16. The compositional dependence of the isomer shifts in $NaMn(Fe_{1-x}In_x)_2(PO_4)_3$.

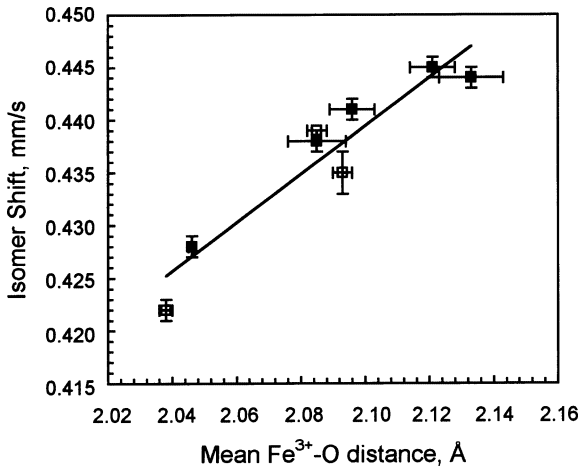

FIGURE 17. The relationship between the 295 K isomer shift and the mean Fe^{3+}-O distance in $NaMn(Fe_{1-x}In_x)_2(PO_4)_3$, solid squares, and in $NaFe_{3.67}(PO_4)_3$ (Korzenski et al. 1998), $Na_{0.5}Li_{0.5}MnFe_2(PO_4)_3$ (Hermann et al. 2001) and $Ag_2Mn_2Fe(PO_4)_3$ (Chouaibi et al. 2001), open squares.

ACKNOWLEDGMENTS

The authors acknowledge the financial support of the Fonds National de la Recherche Scientifique, Belgium, for grant 9.4565.95 and for a visiting professorship for GJL during the 2000–2001 academic year.

REFERENCES CITED

Antenucci, D. (1992) Synthèse et cristallochimie de composés à structure alluaudite. Incidences dans les processus d'altération des phosphates Fe-Mn des pegmatites granitiques. Unpublished Ph. D. Thesis, University of Liège, 259 p.

Antenucci, D., Miehe, G., Tarte, P., Schmahl, W.W., and Fransolet, A.-M. (1993) Combined X-ray Rietveld, infrared and Raman study of a new synthetic variety of alluaudite, $NaCdIn_2(PO_4)_3$. European Journal of Mineralogy, 5, 207–213.

Antenucci, D., Fransolet, A.-M., Miehe, G., and Tarte, P. (1995) Synthèse et cristallochimie de $NaCaCdMg_2(PO_4)_3$, phosphate nouveau à structure alluaudite sans cation trivalent. European Journal of Mineralogy, 7, 175–181.

Burnham, C.W. (1991) LCLSQ version 8.4, least-squares refinement of crystallographic lattice parameters. Department of Earth and Planetary Sciences, Harvard University.

Černý, P. (1991) Rare-element granitic pegmatites. Part I: Anatomy and internal evolution of pegmatite deposits. Geoscience Canada, 18, 49–67.

Chouaibi, N., Daidouh, A., Pico, C., Santrich, A., and Veiga, M.L. (2001) Neutron diffraction, Mössbauer spectrum, and magnetic behavior of $Ag_2FeMn_2(PO_4)_3$ with alluaudite-like structure. Journal of Solid State Chemistry, 159, 46–50.

De Grave, E. and Van Alboom, A. (1991) Evaluation of ferrous and ferric Mössbauer fractions. Physics and Chemistry of Minerals, 18, 337–342.

Ercit, T.S., Hawthorne, F.C., and Černý, P. (1986) The crystal structure of bobfergusonite. Canadian Mineralogist, 24, 605–614.

Farmer, V.C. (1974) The infrared spectra of minerals. Mineralogical Society Monographs, 4, 539 p.

Hartmann-Boutron, F. and Imbert, P. (1968) Mössbauer study of the electronic and magnetic properties of Fe^{2+} done in some spinel-type compounds. Journal of Applied Physics, 39, 775–784.

Hatert, F., Keller, P., Lissner, F., Antenucci, D., and Fransolet, A.-M. (2000) First experimental evidence of alluaudite-like phosphates with high Li-content: the $(Na_{1-x}Li_x)MnFe_2(PO_4)_3$ series (x = 0 to 1). European Journal of Mineralogy, 12, 847–857.

Hatert, F., Antenucci, D., Fransolet, A.-M., and Liégeois-Duyckaerts, M. (2001) The crystal chemistry of lithium in the alluaudite structure: a study of the $(Na_{1-x}Li_x)CdIn_2(PO_4)_3$ solid solution (x = 0 to 1). Journal of Solid State Chemistry, in press. **{{auth: update?}}**

Herber, R.H. (1984) Structure, bonding, and the Mössbauer lattice temperature. In R.H. Herber, Ed., Chemical Mössbauer Spectroscopy, p. 199. Plenum Press, New York.

Hermann, R.P., Hatert, F., Fransolet, A.-M., Long, G.J., and Grandjean, F. (2001) Mössbauer spectral evidence for next-nearest neighbor interactions within the alluaudite structure of $Na_{1-x}Li_xMnFe_2(PO_4)_3$. Solid State Sciences, in press. **{{auth: update}}**

Ingalls, R. (1964) Electric-Field Gradient Tensor in Ferrous Compounds. Physical Review 133, A787–A795.

Khorari, S., Rulmont, A., and Tarte, P. (1997) Alluaudite-like structure of the arsenate $Na_3In_2(AsO_4)_3$. Journal of Solid State Chemistry, 134, 31–37.

Korzenski, M.B., Schimek, G.L., Kolis, J.W., and Long, G.J. (1998) Hydrothermal synthesis, structure, and characterization of a mixed-valent iron (II/III) phosphate, $NaFe_{3.67}(PO_4)_3$: a new variation of the alluaudite structure type. Journal of Solid State Chemistry, 139, 152–160.

Leroux, F., Mar, A., Payen, C., Guyomard, D., Verbaere, A., and Piffard, Y. (1995a) Synthesis and structure of $NaMn_3(PO_4)(HPO_4)_2$, an unoxidized variant of the alluaudite structure type. Journal of Solid State Chemistry, 115, 240–246.

Leroux, F., Mar, A., Guyomard, D., and Piffard, Y. (1995b) Cation substitution in the alluaudite structure type : synthesis and structure of $AgMn_3(PO_4)(HPO_4)_2$. Journal of Solid State Chemistry, 117, 206–212.

Lii, K.-H. and Ye, J. (1997) Hydrothermal synthesis and structure of $Na_3In_2(PO_4)_3$ and $Na_3In_2(AsO_4)_3$: synthetic modifications of the mineral alluaudite. Journal of Solid State Chemistry, 131, 131–137.

Long, G.J., Hautot, D., Grandjean, F., Meisner, G.P., and Morelli, D.T. (2000) Reply to Comment on Mössbauer effect study of filled antimonide skutterudites. Physical Review B, 62, 6829–6831.

Moore, P.B. (1971) Crystal chemistry of the alluaudite structure type: Contribution to the paragenesis of pegmatite phosphate giant crystals. American Mineralogist, 56, 1955–1975.

Moore, P.B. and Ito, J. (1979) Alluaudites, wyllieites, arrojadites: crystal chemistry and nomenclature. Mineralogical Magazine, 43, 227–235.

Moore, P.B. and Molin-Case, J. (1974) Contribution to pegmatite phosphate giant

crystal paragenesis: II. The crystal chemistry of wyllieite, $Na_2Fe^{2+}_2Al(PO_4)_3$, a primary phase. American Mineralogist, 59, 280–290.

Rulmont, A., Cahay, R., Liégeois-Duyckaerts, M., and Tarte, P. (1991) Vibrational spectroscopy of phosphates: some general correlations between structure and spectra. European Journal of Solid State and Inorganic Chemistry, 28, 207–219.

Shannon, R.D. (1976) Revised effective ionic radii and systematic studies of interatomic distances in halides and chalcogenides. Acta Crystallographica, A32, 751–767.

Shinno, I. and Li, Z. (1998) Octahedral site Fe^{2+} quadrupole splitting distributions from the Mössbauer spectra of arrojadite. American Mineralogist, 83, 1316–1322.

Tang, X., Jones, A., Lachgar, A., Gross, B.J., and Yarger, J.L. (1999) Synthesis, crystal structure, NMR studies, and thermal stability of mixed iron-indium phosphates with quasi-one-dimensional frameworks. Inorganic Chemistry, 38, 6032–6038.

Ungethüm, H. (1965) Eine neue Methode zur Bestimmung von Eisen(II) in Gesteinen und Mineralen, insbesondere auch in bitumenhaltigen Proben. Zeitschrift für angewandte Geologie, 11, 500–505.

Vandenberghe, R.E. and De Grave, E. (1989) Mössbauer effect studies of oxidic spinels. In G.J. Long and F. Grandjean, Eds., Mössbauer Spectroscopy Applied to Inorganic Chemistry, vol. 3, p. 59–182, Plenum Press, New York.

Warner, T.E., Milius, W., and Maier, J. (1993) Synthesis and structure of $Cu_{1.35}Fe_3(PO_4)_3$ and $Cu_2Mg_3(PO_4)_3$: new mixed valence compounds of the alluaudite structure type. Journal of Solid State Chemistry, 106, 301–309.

White, B.W. and Keramidas, V.G. (1972) Vibrational spectra of oxides with the *C*-type rare earth oxide structure. Spectrochimica Acta, 28A, 501–509.

Yakubovich, O.V., Simonov, M.A., Egorov-Tismenko, Y.K., and Belov, N.V. (1977) The crystal structure of a synthetic variety of alluaudite, $Na_2(Fe^{3+}_{0.5}Fe^{2+}_{0.5})_2Fe^{2+}[PO_4]_3$. Soviet Physics Doklady, 22(10), 550–552.

Young, R.A., Larson, A.C., and Paiva-Santos, C.O. (1998) User's guide to program DBWS-9807 for Rietveld analysis of x-ray and neutron powder diffraction patterns. School of Physics, Georgia Institute of Technology, Atlanta, U.S.A., 56 p.

MANUSCRIPT RECEIVED JANUARY 15, 2002
MANUSCRIPT ACCEPTED JULY 24, 2002
MANUSCRIPT HANDLED BY BYRAN CHAKOUMAKOS